Production of biodegradable PLGA foams processed with high pressure CO_2

Álvarez, I. [a], Gutiérrez, C. [b], Rodríguez, J.F. [a], de Lucas, A. [a], García, M.T.[a], *

[a,] Department of Chemical Engineering. University of Castilla-La Mancha. Facultad de C.C. Químicas. Avda. Camilo José Cela 12, 13071 Ciudad Real, Spain.

[b] AMBLING Ingeniería y Servicios. Cáceres, Plasencia, Spain.

[*]Corresponding author:

e-mail: Teresa.García@uclm.es

Phone: +34926295300/5311

Fax: +34926295256

Abstract

Microcellular scaffolds were prepared using high pressure fluids. Solutions of biodegradable material Poly (lactic-co-glycolic) acid (PLGA) in a green solvent such as ethyl lactate was used as the scaffold matrix. To carry out polymer foaming from polymer solutions allows the possibility of reducing the working temperature. The effect of the ratio lactide to glycolide of the polymer, the working pressure, the initial concentration of the polymer in the solvent and the depressurization time were the variables studied at a temperature of 25 °C. The morphology of the foams obtained was characterized based on the cell diameter and its standard deviation, indicator of the homogeneity of the scaffolds obtained, as well as the density of cells. In addition, a study was performed on how the glass transition temperature (Tg) of a polymer is modified by the plasticizing effect of CO_2 pressure.

32

33

1. Introduction

In recent years, the use of biopolymers in tissue engineering has increased thanks to their high biocompatibility which make them suitable for its use as controlled release systems. Their use has also been enhanced due to environmental issues and the fact that they are obtained from renewable raw materials [1]. Other key properties of these biomaterials are their antibacterial activity and biodegradability [2], which cause immune or toxic reactions to be reduced when they are implanted in the human body [3, 4]. In addition, these biopolymers can be chemically modified by adjusting their degradation rate to the process for which they have been designed, as well as maintaining the mechanical and electrical properties required in their specific application [5-7].

The material of first choice of researches for tissue engineering and drug delivery systems is the group comprising by the poly (α-hidroxy acids): polylactic acid, polyglycolic acid and their copolymer, poly (lactic-co-glycolic) acid [8-11]. This biodegradable polyester family has been regarded as one of the few synthetic biodegradable polymers with controllable biodegradability, excellent biocompatibility and high safety [12]. Moreover, it has been approved by the Food and Drug Administration (FDA) for its use in tissue engineering [13].

Traditional synthesis methods of controlled release systems use organic solvents in which both the polymer and the pharmaceutical compound are dissolved. Most of these solvents are toxic and they must be eliminated from the device before being implanted in the organism [14-17]. These methods require additional stages of heating that can lead to the

55 degradation of bioactive compounds [18]. The mentioned disadvantages are the main reason

56 to develop innovative methodologies for the synthesis of controlled release systems that can

57 be used in tissue engineering. One of these methodologies is supercritical fluid (SCF) or high

58 pressure technology. The use of green physical blowing agents, such as gaseous or

59 supercritical CO_2/N_2 has been well established in the manufacture of foam product. The

60 employment of supercritical and high pressure fluids, especially supercritical carbon dioxide, is a

61 powerful alternative to carry out polymer foaming and impregnation process because of the lack

62 of residual solvent in the final products [19, 20]. Supercritical carbon dioxide ($scCO_2$) is proposed

63 as one of the most suitable solvents in gas foaming processes because its critical point is easy to

64 reach ($T_c = 31.1$ °C, $P_c = 73$ bar) is non-flammable, non-toxic, inert and it leaves no residues after

65 its evaporation. Using supercritical and high-pressure CO_2, the gas molecules are absorbed into

66 the polymer matrix until saturation, causing a decrease in the glass transition temperature (T_g) of

67 the polymer. If depressurization takes place, bubbles are induced to form and grow. As the CO_2

68 concentration decreases, the glass transition temperature begins to rise again and the pores formed

69 by the nucleation of the CO_2 bubbles become permanent giving rise to the formation of a

70 microcellular foam [21, 22]. Table 1 shows a summary of working pressures and temperatures of

71 other investigations to carry out the foaming of biodegradable polymers. The properties of the

72 polymer and its blowing agent under high pressure and temperature have a great influence on the

73 properties of the created porous structure.

74

75

76

77

78

79 Table 1. Literature review summary on the foaming conditions for PLGA in $scCO_2$.

Polymer	Temperature (°C)	Pressure range (bar)	Contact time range (h)	Depressurization rate or time	Refs.
PLGA5050	-	55.2	24	-	[23]

PLGA	35, 100	103 - 276	0.3	0.3-0.4 MPa/s	[24]
PLGA8020 PLGA6535	35		24	10-12 s	[21]
PLGA	35-55	75-150		0.1-6 MPa/min	[25]
PLGA5050	25	20	0.1	-	[26]
PLGA8515	35-65	150-200	2	20 bar/s	[27]
PLGA5050	50	250	6	80 bar/min	[28]
PLGA5050	27	60	0.5	5 bar/min	[29]
PLGA	33-42	80-200	2-8	0.25 – 1 bar/s	[30]
PLGA	40	180	1	3-90 min	[31, 32]

80

81   Some studies have confirmed that using polymers in solution to carry out foaming,

82 allows working at a lower temperature [33, 34]. This avoids the degradation of the drug when

83 it is impregnated in the polymeric device. In this way, it is a key factor to find solvents that

84 are suitable for its use in the pharmaceutical industry and whose characteristics are not

85 harmful to human health. FDA establishes the suitability of the employment of some typical

86 solvents in drug formulations. Within this classification, Class 3 solvents are the least toxic,

87 e.g. acetone, ethyl acetate and some short chain alcohols. Previous researches of the group have

88 shown the good solubility of ethyl acetate and ethyl lactate in CO_2 making it viable to carry out

89 foaming and drug saturation at mild temperature [35]. In this work, we have focus in the use of

90 ethyl lactate as solvent. It is accepted as Generally Recognized As Safe (GRAS) and recently

91 approved by FDA as a pharmaceutical and food additive [36].

92   The aim of this work is to study the influence of different operating variables (ratio PLA

93 to PGA of the polymer, pressure, initial concentration of PLGA in the solution and

94 depressurization time) on the foaming of PLGA solutions in ethyl lactate using CO_2 at high

95 pressure as foaming gas in order to develop customizable structures that can be used as controlled

96 release systems.

2. Materials and methods

2.1. Materials

Materials were used as received from suppliers. Polymeric foams were synthesized from Poly (lactic-co-glycolic) acid (PLGA). Two different monomer ratio lactide: glycolide were studied in this work: PLGA5050 (50 mol % lactic acid, 50 mol % glycolic acid) and PLGA7525 (75 mol % lactic acid, 25 mol % glycolic acid) with a Mw = 17,000 g/mol as polystyrene-equivalent molecular weight value measured using GPC chromatography. These polymers were supplied by Corbion Purac (Netherlands). Ethyl lactate was purchased from Sigma-Aldrich and used as received. Carbon dioxide with a purity of 99.8% was supplied by Carburos Metálicos S.A. (Spain).

2.2. Experimental setup and procedure for measurement of glass transition temperature at high pressures

Differential scanning calorimetry (DSC) is the most effective technique for determining the glass transition temperature of a polymer. In this work, a High Pressure SENSYS evo DSC (Setaram, Madrid) is used to study the thermal behaviour of PLGA at high pressures. The equipment and procedure were described elsewhere [37]. The melting point (T_m = 156.6 ∘C) and enthalpies of indium were used for temperature and heat capacity calibration. The system was pressurized using an ISCO 260D syringe pump up to the desired pressure. High pressure Inconel crucibles enabled measurements up to 400 bar. Samples were placed in the crucibles and weighted previously to be sealed with the cell. After that, samples were annealed at the desired pressure for 24 hours to ensure the total CO_2 sorption. DSC scans were made using an initial heating at 10 °C/min up to 100 °C to release thermal and sorption history, and to provide better fit in the crucible. The samples were then annealed for 10 min, cooled at the same rate down to 0°C by using a stream of liquid nitrogen and annealed for another 10 min. T_g measurements were carried

122   out during the second heating, and it is identified from the change in heat flow resulting from a

123   change in heat capacity at the transition temperature of the polymer during each scan.

124

125   ## 2.3. Experimental foaming setup and experimental procedure

126   Foaming experiments were carried out in a homemade batch-type high-pressure vessel

127   described elsewhere [34]. It is a 316-stainless-steel high-pressure vessel with a volume of 350

128   mL. It consisted in three main modules: (i) pressurization module with a heater exchanger (JP

129   Selecta Frigiterm 6000382, Spain) to cool the CO_2 in order to assure liquid state and a pump

130   (Milton Roy–Mil Royal D, France) to pressurize the system; (ii) high-pressure vessel module with

131   the high-pressure vessel. To heat up the system a digital controller regulated the electric current

132   through a resistance which was placed around the vessel; (iii) depressurization module with a

133   discharge valve and a gas metre model Ritter TG-05 (±0.005 L).

134   To produce microporous scaffolds, a certain amount of PLGA was dissolved in ethyl

135   lactate and the solution was placed in the vessel. Initial concentration for both monomers ratio

136   lactide:glycolide of the polymer, PLGA5050 or PLGA7525, in ethyl lactate was 0.4 g

137   polymer/mL solvent or 0.8 g polymer/ mL solvent. The vessel was then filled with CO_2 until the

138   working pressure. This CO_2 was cooled and compressed by a positive-displacement pump. The

139   pressure was regulated by a back-pressure regulator (BPR) and checked by a manometer.

140   Temperature and pressure were kept constant for 24 hours to promote the formation of a

141   homogeneous microcellular structure and ensure total solvent solubilization in the CO_2 rich-

142   phase. Previously, a series of experiments were carried out at shorter and longer contact times

143   with CO_2 inside the vessel, establishing that the minimum time to ensure total sorption of the gas

144   and solubility of the solvent in it was 24 hours. Then, the vessel was vented by opening the

145   discharge valve that was controlled manually by the measurement of the flow in the turbine flow

146   meter.

147

148 **2.4. Foam characterization**

149 Cell structure and morphology were studied by scanning electron microscopy (SEM)

150 using a Quanta 250 equipment with a wolfram filament operating at a working potential of 10 kV

151 (FEI Company). Motic Images 2.0 software was used to analyse mean cell size and homogeneity

152 calculated from the standard deviation of the sample based on the SEM images. Also cell density

153 was determined. It is defined as the number of cells of foamed sample per unit volume of the

154 original polymer. Cells density was calculated according to the following expression:

155
$$Cells\ density\ \left(\frac{cells}{cm^3}\right) = \left(\frac{n \cdot M^2}{A}\right)^{3/2} \qquad (1)$$

156 where n is the number of cells in the micrograph, A the area of the micrograph (cm^2) and M the

157 magnification factor [38, 39].

158 The residual amount of solvent present in the foams was determined by

159 thermogravimetric analysis (TA-DSC Q 600). All analyses were carried out in a nitrogen

160 atmosphere with a flow rate of 100 ml/min. Weight loss due to solvent volatilization (~150 ºC)

161 and polymer degradation (~325 ºC) was recorded in the thermograph as a function of temperature.

162 The samples (3-10 mg) were heated up to 450 ºC at a heating rate of 40 ºC/min. The data were

163 analysed with the universal analysis software TA 2000.

164

165 # 3. Results and discussion

166 ## 3.1. Variation of glass transition temperature (T_g) at high CO_2 pressure

167 As the molecules of CO_2 are absorbed into the polymer matrix, the chains swell,

168 increasing the free volume. In addition, this phenomenon causes the plasticization of the polymer

169 and the reduction of its glass transition temperature [40]. In this way, because of the swelling, the

170 diffusion of small drugs molecules into polymer matrix is enhanced [41] and a homogeneous

171 impregnation of the scaffold is favoured. Kasturirangan et al. [41] state that polymers that contain

172   carbonyl groups in its structure interacts strongly with CO_2 thus increasing the solubility of this

173   gas in polymers matrix such as poly(methyl metracrylate) (PMMA) more than in polymers

174   without C=O groups such as polystyrene (PS) or poly(vinyl chloride) (PVC). For this reason, the

175   glass transition temperature of PLGA is expected to be reduced because of the effect of high-

176   pressure CO_2.The variation of glass transition temperature of PLGA because of CO_2 sorption is

177   shown in Figure 1. PLGA formula has been included in Figure 1 in order to check its chemical

178   structure and the presence of carbonyl groups.

179
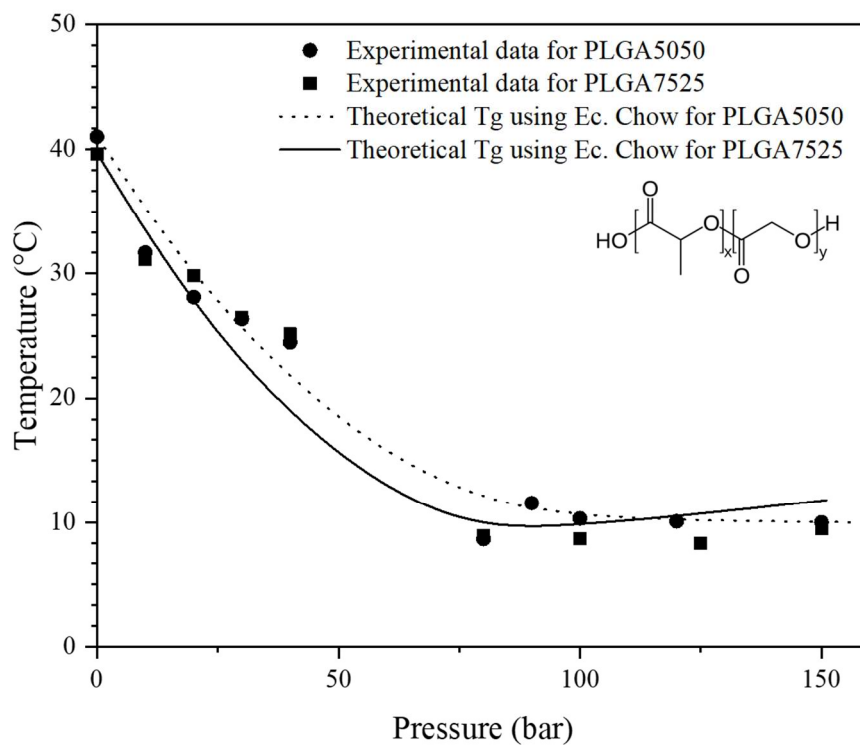
180

181   Figure 1. Variation of glass transition temperature of (●) PLGA5050 and (■) PLGA7525.

182   Prediction of the decrease of T_g of (- - -) PLGA5050 and (—) PLGA7525 using Chow's equation.

183

184

185   Regarding the experimental data obtained, a decrease of the T_g from 42 °C at ambient

186   pressure until 20 °C at pressures below the critical pressure of the CO_2 is observed. At pressures

187 above 70 bar, the T_g of the polymers do not decrease linearly but it is maintained almost at around

188 10 °C for both ratios PLA to PGA. This may be due to the fact that at pressures above the critical

189 pressure of CO_2, the polymer matrix is saturated with the gas molecules. Because of that, the

190 amount of CO_2 does not increase in the same way as it does at lower pressures. [35, 42, 43]. [35,

191 42, 43]. The equilibrium concentration of CO_2 in the polymer, at a constant pressure, is composed

192 of dissolution and sorption of the gas, as described the "dual sorption and transport model". The

193 plasticization effect by high-pressure carbon dioxide seems to promote the pressure dependence

194 of the sorption and transport coefficients [44].

195   In order to know if the presence of the solvents modifies the glass transition temperature

196 of PLGA at high pressure, further experiments were performed in the high-pressure DSC. In

197 Figure 2, the experimental data obtained for a concentration of 0.8 g PLGA/mL ethyl lactate and

198 0.4 g PLGA/mL ethyl lactate of both monomers ratio PLA:PGA (PLGA7525 and PLGA5050)

199 are shown.

200
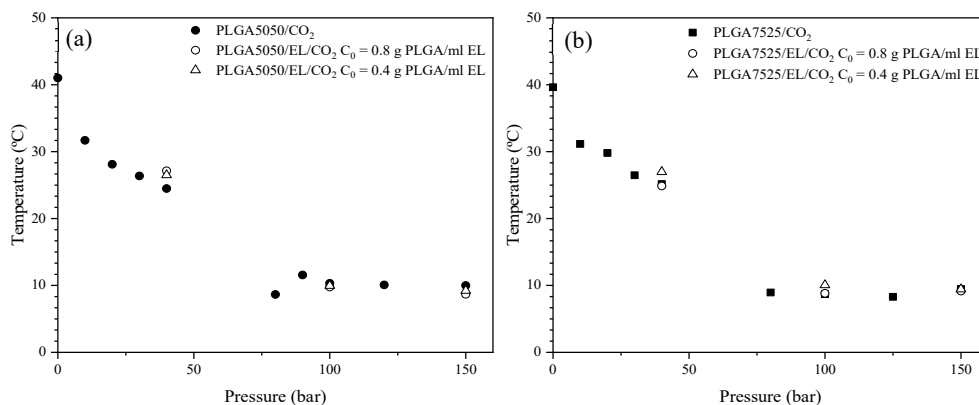
201

202 Figure 2. Variation of glass transition temperature of PLGA in ethyl lactate solutions. Figure (a):

203 (●) PLGA5050; (○) Initial concentration: 0.80 g PLGA5050/mL ethyl lactate; (△) Initial

204 concentration: 0.40 g PLGA5050/mL ethyl lactate. Figure (b): (■) PLGA7525; (○) Initial

205 concentration: 0.80 g PLGA7525/mL ethyl lactate; (△) Initial concentration: 0.40 g

206 PLGA7525/mL ethyl lactate.

207

208   Comparing the results obtained for the T_g values in the case of PLGA and ethyl lactate

209   polymeric solutions with those reported previously in Figure 1, it can be established that the

210   presence of the solvent does not significantly affect the glass transition temperature of the

211   polymer. Because of CO_2 sorption in the polymers, the matrix is expanded leading to an increase

212   in the free volume of the polymer. In that way, small molecules soak easily through the matrix

213   than the bigger ones [37]. The great impact of CO_2 on PLGA glass transition temperature causes

214   that the presence of ethyl lactate does not alter the properties of the polymer when exposed to CO_2

215   at elevated pressure. Stafford et al. [45] also confirm that the presence of low molecular weight

216   substances in a polymer/CO_2 system does not affect the value of the T_g observed.

217   Chow's equation for polymer-diluent mixtures [46] has been used to correlate the

218   decrease of T_g from ambient pressure to 150 bar. The sorption of CO_2 into the polymer matrix

219   promote the plasticization resulting in a lower T_g. Chow derived an equation for predicting this

220   effect:

221
$$\ln\left(\frac{T_g}{T_{g,0}}\right) = \beta \cdot [\theta \cdot \ln\theta + (1 - \theta) \cdot \ln(1 - \theta)] \tag{2}$$

222
$$\theta = \frac{M_m}{z \cdot M_d} \cdot \frac{w_1}{1 - w_1} \tag{3}$$

223
$$\beta = \frac{z \cdot R}{M_m \cdot \Delta C_{pp}} \tag{4}$$

224

225   where T_g is the glass transition temperature of the polymer under pressure; $T_{g,0}$ is the glass

226   transition temperature of the pure polymer at atmospheric pressure; θ, β are a nondimensional

227   parameters defined in expressions (2) and (3); M_m is the molar mass of the monomeric unit which

228   makes up the polymer ; M_d is the molar mass of the dissolved gas; R is the gas constant; w_1 is the

229   weight fraction of CO_2 in the polymer mixture; ΔC_{pp} is the excess transition isobaric specific heat

230   of the polymer (These values were obtained from the experimental data minimizing the quadratic

231   error with respect to the theoretical data) and z is the lattice coordination number which can be

232   either 1 or 2. The lattice coordination number z represents the number of macromolecules in

233   contact with a single CO_2 molecule [47] and it depends on the nature of the polymer. In our study,

234   this parameter was set to 2 because better fit with experimental data was obtained. However, some

235   researches stablish that when z is two or greater a retrograde vitrification of the polymer is present

236   but in the experimental runs no retrograde vitrification was noticed. Reignier et al. [48] compared

237   the results of Chow model with both values. For z = 1 some experimental points were

238   underestimated and for z = 2 it seemed to be able to estimate the experimental points. Theoretical

239   glass transition temperature using Chow's equation fits experimental data acceptably well

240   independently of the ratio PLA to PGA of the polymers. Measurement tests were done in duplicate

241   with an error lower than 0.34 °C for all the experiments. No reproducibility was obtained around

242   the critical point of the gas while having to refuse these experimental points. The values of all the

243   parameters used have been included in Table 2.

244

245   Table 2. Parameters of Chow's equation.

M_m	130 g/mol
M_d	44.01 g/mol
Z	2
ΔC_{pp} (PLGA7525)	0.864 J/g·K
ΔC_{pp} (PLGA5050)	0.848 J/g·K
$T_{g,0}$ (PLGA7525)	39.63 °C
$T_{g,0}$ (PLGA5050)	41.02 °C

246

247   3.2. Foaming experiments

248   Table 3 shows the experimental runs carried out in order to stablish the influence of the

249   ratio PLA:PGA of the polymers, the initial concentration of the polymers in the solvent, the

250   pressure and the depressurization time in the internal structure of the foamed samples. Two

251   different levels were selected for each factor. Cells size, cells density and their standard deviation

252   of the foams is also included in Table 3. All the experiments were accomplished according the

253   same experimental procedure at 25 °C and a contact time inside the vessel of 24 hours to ensure

254   total CO_2 sorption.

255

256   Table 3. Experimental runs and characterization of PLGA foams: cells size and cells density.

Run	Ratio PLA:PGA	Pressure (bar)	Initial concentration (g PLGA/ml EL)	Dep. time (min)	Cells size (µm)	Standard Deviation (µm)	Cells density (cells/cm^3)	Standard Deviation (cells/cm^3)
1	5050	80	0.4	15	458.76	165.22	2.59E+04	8.63E+03
2	5050	120	0.4	15	398.26	105.90	2.37E+04	3.52E+03
3	5050	80	0.8	15	287.11	179.88	2.56E+04	7.11E+03
4	5050	120	0.8	15	297.04	69.32	3.33E+04	2.03E+03
5	5050	80	0.4	30	496.21	109.26	2.99E+04	4.06E+03
6	5050	120	0.4	30	325.21	87.23	2.66E+04	2.55E+03
7	5050	80	0.8	30	265.59	124.45	1.06E+04	3.29E+03
8	5050	120	0.8	30	219.40	50.14	3.99E+04	1.97E+03
9	7525	80	0.4	15	-	-	-	
10	7525	120	0.4	15	387.41	147.77	1.46E+04	6.64E+03
11	7525	80	0.8	15	365.11	89.65	1.25E+04	1.57E+03
12	7525	120	0.8	15	321.07	65.35	1.83E+04	2.62E+03
13	7525	80	0.4	30	562.50	146.36	9.53E+03	8.81E+02
14	7525	120	0.4	30	299.98	98.85	2.85E+04	1.44E+03
15	7525	80	0.8	30	321.05	125.36	1.83E+04	5.03E+03
16	7525	120	0.8	30	387.56	71.21	2.40E+04	7.22E+03

257

258

259   Figure 3 illustrates cell size and cell density obtained for those experiments in which

260   PLGA foaming was successfully achieved. These parameters are the most important ones when

261   studying the influence of the different factors on the final foam structure obtained. Furthermore,

262   the analysis of the standard deviation of each experiment indicates the degree of homogeneity of

263   the foams formed. A smaller deviation results in a greater homogeneity. According with Table 3,

264   the lower cells size is obtained for Run 8 where higher pressure, initial concentration of the

265   polymer on the solvent and depressurization time was employed.

266

267
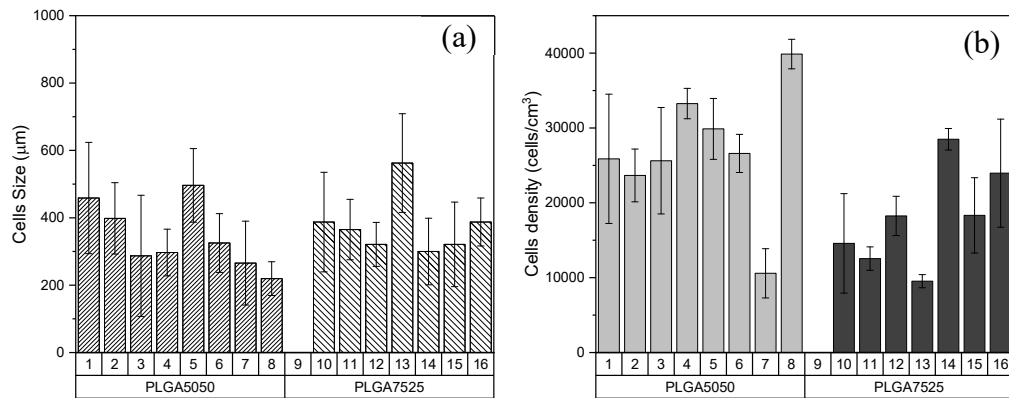
Figure 3. Average cells size (a) and cells density (b) of runs 1-16 for PLGA5050 and PLGA7525 using ethyl lactate as solvent.

In controlled release systems it is important to obtain a homogeneous pore distribution with an adequate size to allow the impregnation of bioactive compounds and to avoid different rates of drug release maintaining a controlled one over time. The desired pore size depends on the specific application of the foams. In the case of unimpregnated scaffolds for tissue regeneration and cell growth, higher pore sizes and a highly interconnected network are required, which can stimulate cell infiltration and allow for the adequate exchange of nutrients and metabolic residues through the scaffolding [49, 50]. In the synthesis of controlled release systems, smaller pore sizes are preferred to obtain sustained drug concentrations within the therapeutic interval [51].

Table 4 summarizes the residual amount of solvent as well as the glass transition temperature measurements after foaming experiments of each of the foams formed. By means of thermogravimetric analysis, the amount of solvent present in the foams was measured, but in all cases did not exceed 3%, except in experiment 9 in which a dry microcelular foam was not achieved. Further experiments showed that these residual amounts of solvents could be removed by adding an extra stream of CO_2 at the end of the depressurization stage [34].

287   Table 4. Residual final concentration of solvent in the foams and glass transition temperature (T_g).

Run	Ratio PLA:PGA	Pressure (bar)	Initial concentration (g PLGA/mL solvent)	Depressurization time (min)	Residual solvent (% wt)	T_g (°C)
1	5050	80	0.4	15	1.29	38.55
2	5050	120	0.4	15	1.05	38.15
3	5050	80	0.8	15	2.24	38.07
4	5050	120	0.8	15	1.12	39.67
5	5050	80	0.4	30	1.05	39.69
6	5050	120	0.4	30	0.67	39.01
7	5050	80	0.8	30	0.69	39.65
8	5050	120	0.8	30	0.39	40.81
9	7525	80	0.4	15	-	-
10	7525	120	0.4	15	1.81	40.64
11	7525	80	0.8	15	2.60	39.88
12	7525	120	0.8	15	1.35	40.98
13	7525	80	0.4	30	3.01	39.42
14	7525	120	0.4	30	0.66	41.52
15	7525	80	0.8	30	1.23	40.23
16	7525	120	0.8	30	0.84	41.14

288

289

290   Figure 4 represents an example of thermogravimetric analysis for these experiments. In

291   this Figure, it is possible to observe the degradation peaks corresponding to ethyl lactate and

292   PLGA polymer. Longer depressurization times get a reduction of the residual solvent. The

293   advantage of using ethyl lactate as a solvent is that even if small residual traces would be remained

294   in the foam, structure of the scaffolds will not be affected. The glass transition temperature did

295   not vary significantly over the initial one of the polymer flakes, thus remaining above body

296   temperature.   Consequently, it can be concluded that these foams are suitable for its

297   implementation in the organism as controlled release systems.

298

299
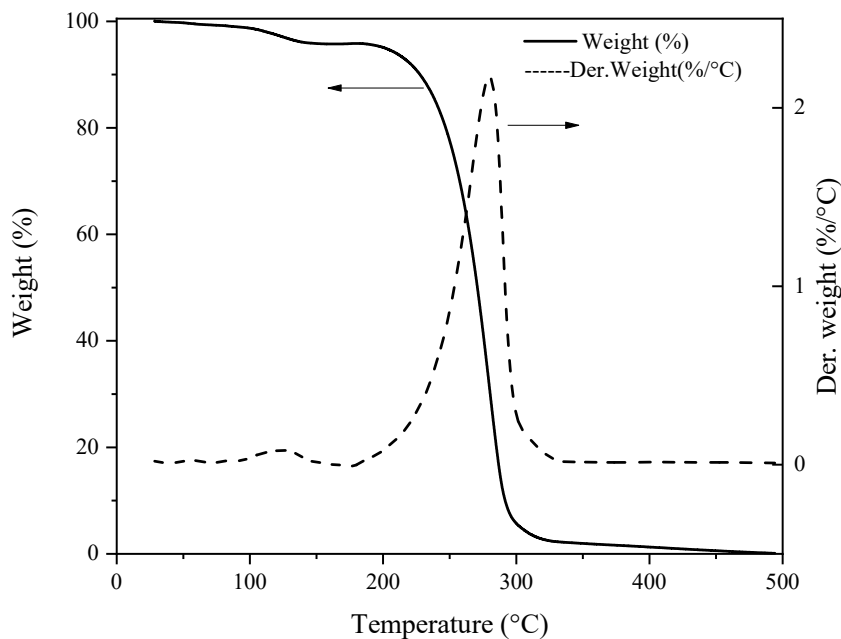
Figure 4. Thermogravimetric analysis for Run 2 using the software TA Universal. The

degradation peaks corresponding to solvent and polymer are shown.

302

The effect of the PLA:PGA ratio on foams should be compared in experiments conducted

under the same operating conditions. Figure 5 represents SEM images of the internal structure of

foams obtained in runs 8 and 16 performed at 120 bar, 0.8 g PLGA/ml ethyl lactate and a

depressurization time of 30 minutes. According to Table 3, in general, the experiments in which

the polymer used was PLGA7525 have a larger cell diameter than PLGA5050 due to better CO_2

diffusion. Some authors claim that the stearic hindrance close to the carbonyl group and the higher

free volume of the methyl groups modify the solubility and interaction between the polymeric

matrix and the CO_2. Higher glycolide content leads to decrease CO_2 sorption resulting in the

formation of smaller cells [32, 43, 52].

312

313
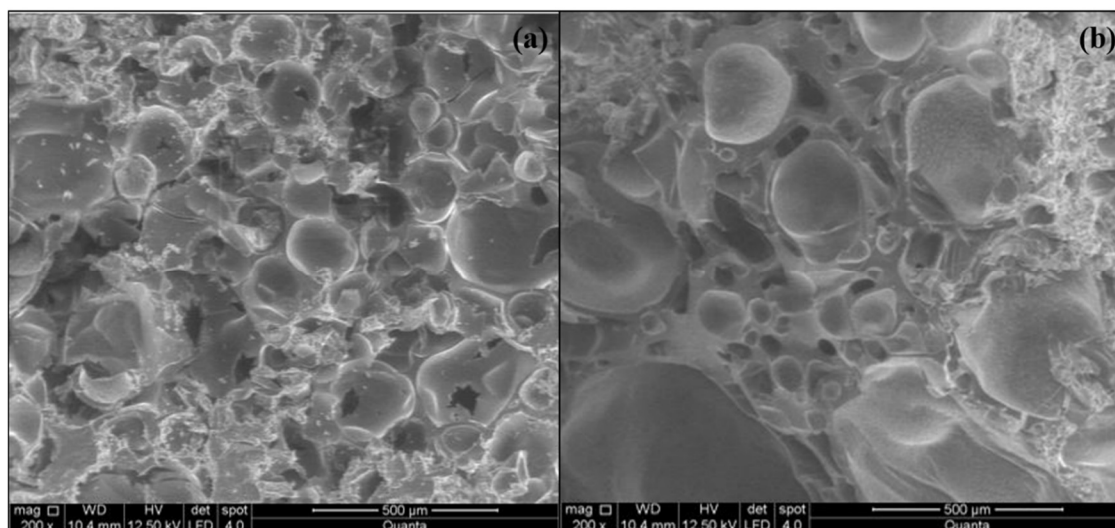
Figure 5. SEM images of the internal structure of the foams. Effect of ratio PLA:PGA on foam

morphology. Operation conditions: Pressure: 120 bar, Initial concentration: 0.8 g PLGA/ml ethyl

lactate, Depressurization time: 30 min. (a) PLGA5050, (b) PLGA7525.

The effect of an increase in working pressure on the foam structure should lead to a

decrease in cell diameter and a more homogeneous distribution, as well as an increase in cell

density [19, 53]. There was no clear trend in the pressure range studied when this increase in

pressure occurs. This may be due because the gas density value at both working conditions is

similar. The density of CO_2 at 25 ºC and 80 bar is, approximately, 779 g/L and 25 ºC and 120 bar

is 846 g/L. In that way, a great difference in the internal structure of the foams was not noticeable,

although a slight decrease in cell size can be observed in the experiments carried out at 120 bar.

The most significant effect of the pressure can be seen in the residual amount of solvent remaining

in the foams after the depressurisation stage. In all cases, an increase in pressure resulted in drier

foams as the solubility of the ethyl lactate in CO_2 increases with increasing pressure [36, 54, 55].

This is the result of the fact that at higher pressures, the amount of solvent that can be solubilized

in the CO_2-rich phase is higher, resulting in a drier scaffold [35]. To work at even higher pressures,

it would not be necessary to use an extra CO_2 stream to eliminate possible traces of solvent [56].

The effect of the initial concentration of the polymer in the solution, regardless of the

lactide:glycolide ratio used, showed that higher initial concentration causes the cell size obtained

333 to be smaller, and cells density to increase. These results are in agreement with those obtained by

334 Kiran et al. [53]. In addition, in experiment 9, no foam was obtained since the amount of solvent

335 remained after 24 hours of contact was very high. Previous researches observed that, although the

336 solubility of a solvent in polymer solutions in contact with supercritical carbon dioxide is higher

337 when the initial concentration is lower [35, 57], foaming conditions caused a saturation of ethyl

338 lactate in the CO_2-rich phase inside the vessel. This led to the experiments with an initial

339 concentration of 0.4 g PLGA/mL ethyl lactate to have a larger cell diameter and a higher amount

340 of solvent at the end of the foaming process.

341 Finally, the effect of increasing depressurization time results in a decrease in cell size. At

342 low depressurization rates the CO_2 absorbed in the solution was slowly removed, decreasing the

343 size of the cells and increasing the cells density. This trend is contrary to what is found in the

344 literature, where a shorter depressurization time causes the formation of smaller cells [52, 58-60].

345 Rapid depressurization results in rapid cooling leading to the collapse of the pore walls [61].

346 Faster cooling rate involves a rapid increase in the polymer matrix viscosity and glass transition

347 temperature, which prevents the break of pores walls resulting in a smaller cell size [32].

348

4. Conclusions

350 In this work it has been demonstrated how the plasticizing effect of CO_2 at high pressure

351 reduces the glass transition temperature of PLGA because of the gas molecules sorption in the

352 polymeric matrix. In addition, the use of PLGA solutions in ethyl lactate does not produce a

353 noticeable change in T_g. This plasticization is of vital importance because its causes the chains to

354 swell and, in that way, the diffusion is enhanced and the foaming and impregnation of PLGA is

355 improved.

356 PLGA foaming can be carried out under mild conditions from solutions of this polymer

357 in ethyl lactate. In order to be used as a controlled release system these foams must have a small

358 cell diameter suitable for the impregnation of drugs as well as a homogeneous internal structure.

359 The most suitable operating conditions in order to perform the foaming experiments were found

360   for a lactide:glycolide ratio of 50:50, at high pressure (120 bar), with a high initial concentration

361   of the polymer in the solvent (0.8 g PLGA/mL ethyl lactate) and at high depressurization times.

362   Under these conditions, scaffolds are obtained with a smaller cell diameter and a more

363   homogeneous distribution. In addition, a lower residual amount of solvent in the final foam is

364   obtained.

365

370

5. References

372   [1] L. Yu, K. Dean, L. Li, Polymer blends and composites from renewable resources, Progress in
373   Polymer Science, 31 (2006) 576-602.
374   [2] J.D. Schiffman, C.L. Schauer, A Review: Electrospinning of Biopolymer Nanofibers and their
375   Applications, Polymer Reviews, 48 (2008) 317-352.
376   [3] M. Okamoto, B. John, Synthetic biopolymer nanocomposites for tissue engineering scaffolds,
377   Progress in Polymer Science, 38 (2013) 1487-1503.
378   [4] J.F. Mano, G.A. Silva, H.S. Azevedo, P.B. Malafaya, R.A. Sousa, S.S. Silva, L.F. Boesel,
379   J.M. Oliveira, T.C. Santos, A.P. Marques, N.M. Neves, R.L. Reis, Natural origin biodegradable
380   systems in tissue engineering and regenerative medicine: present status and some moving trends,
381   Journal of The Royal Society Interface, 4 (2007) 999-1030.
382   [5] A.B. Sanghvi, K.P.H. Miller, A.M. Belcher, C.E. Schmidt, Biomaterials functionalization
383   using a novel peptide that selectively binds to a conducting polymer, Nature Materials, 4 (2005)
384   496-502.
385   [6] J.-S. Yang, Y.-J. Xie, W. He, Research progress on chemical modification of alginate: A
386   review, Carbohydrate Polymers, 84 (2011) 33-39.
387   [7] M. Dash, F. Chiellini, R.M. Ottenbrite, E. Chiellini, Chitosan—A versatile semi-synthetic
388   polymer in biomedical applications, Progress in Polymer Science, 36 (2011) 981-1014.
389   [8] L. Brannon-Peppas, Polymers in controlled drug delivery, Medical Plastics and Biomaterials
390   Magazine, (1997).
391   [9] H.K. Makadia, S.J. Siegel, Poly Lactic-co-Glycolic Acid (PLGA) as Biodegradable
392   Controlled Drug Delivery Carrier, Polymers, 3 (2011) 1377-1397.
393   [10] O. Pillai, R. Panchagnula, Polymers in drug delivery, Current opinion in chemical biology,
394   5 (2001) 447-451.
395   [11] R. Thomson, M. Wake, M.J. Yaszemski, A. Mikos, Biodegradable polymer scaffolds to
396   regenerate organs, in: Biopolymers Ii, Springer, 1995, pp. 245-274.
397   [12] F. Asghari, M. Samiei, K. Adibkia, A. Akbarzadeh, S. Davaran, Biodegradable and
398   biocompatible polymers for tissue engineering application: a review, Artificial Cells,
399   Nanomedicine, and Biotechnology, 45 (2017) 185-192.

[13] P. Gentile, V. Chiono, I. Carmagnola, P.V. Hatton, An Overview of Poly(lactic-co-glycolic) Acid (PLGA)-Based Biomaterials for Bone Tissue Engineering, International Journal of Molecular Sciences, 15 (2014) 3640-3659.

[14] R. Arshady, Preparation of biodegradable microspheres and microcapsules: 2. Polyactides and related polyesters, Journal of Controlled Release, 17 (1991) 1-21.

[15] F. Tewes, E. Munnier, B. Antoon, L. Ngaboni Okassa, S. Cohen-Jonathan, H. Marchais, L. Douziech-Eyrolles, M. Souce, P. Dubois, I. Chourpa, Comparative study of doxorubicin-loaded poly(lactide-co-glycolide) nanoparticles prepared by single and double emulsion methods, European journal of pharmaceutics and biopharmaceutics : official journal of Arbeitsgemeinschaft fur Pharmazeutische Verfahrenstechnik e.V, 66 (2007) 488-492.

[16] T.K. Giri, C. Choudhary, A. Alexander, H. Badwaik, D.K. Tripathi, Prospects of pharmaceuticals and biopharmaceuticals loaded microparticles prepared by double emulsion technique for controlled delivery, Saudi Pharmaceutical Journal, 21 (2013) 125-141.

[17] S.H. Oh, S.G. Kang, J.H. Lee, Degradation behavior of hydrophilized PLGA scaffolds prepared by melt-molding particulate-leaching method: comparison with control hydrophobic one, Journal of Materials Science: Materials in Medicine, 17 (2006) 131-137.

[18] A.R.C. Duarte, J.F. Mano, R.L. Reis, Preparation of chitosan scaffolds loaded with dexamethasone for tissue engineering applications using supercritical fluid technology, European Polymer Journal, 45 (2009) 141-148.

[19] E. Reverchon, S. Cardea, Production of controlled polymeric foams by supercritical CO_2, The Journal of Supercritical Fluids, 40 (2007) 144-152.

[20] A.R.C. Duarte, J.F. Mano, R.L. Reis, Supercritical fluids in biomedical and tissue engineering applications: a review, International Materials Reviews, 54 (2009) 214-222.

[21] D.D. Hile, M.L. Amirpour, A. Akgerman, M.V. Pishko, Active growth factor delivery from poly(D,L-lactide-co-glycolide) foams prepared in supercritical CO_2, Journal of Controlled Release, 66 (2000) 177-185.

[22] J.S. Colton, The Nucleation of Microcellular Foams in Semi-Crystalline Thermoplastics, Materials and Manufacturing Processes, 4 (1989) 253-262.

[23] L. Leung, C. Chan, J. Song, B. Tam, H. Naguib, A parametric study on the processing and physical characterization of PLGA 50/50 bioscaffolds, Journal of Cellular Plastics, 44 (2008) 189-202.

[24] K.C. Baker, R. Bellair, M. Manitiu, H.N. Herkowitz, R.M. Kannan, Structure and mechanical properties of supercritical carbon dioxide processed porous resorbable polymer constructs, Journal of the Mechanical Behavior of Biomedical Materials, 2 (2009) 620-626.

[25] X. Xin, Y. Guan, S. Yao, Bi-/multi-modal pore formation of PLGA/hydroxyapatite composite scaffolds by heterogeneous nucleation in supercritical CO_2 foaming, Chinese Journal of Chemical Engineering, 26 (2018) 207-212.

[26] T. Ma, Y.S. Zhang, A.-Z. Chen, J. Ju, C.-W. Gu, R.K. Kankala, S.-B. Wang, Carbon dioxide-assisted bioassembly of cell-loaded scaffolds from polymeric porous microspheres, The Journal of Supercritical Fluids, 120 (2017) 43-51.

[27] X. Xin, Q.Q. Liu, C.X. Chen, Y.X. Guan, S.J. Yao, Fabrication of bimodal porous PLGA scaffolds by supercritical CO_2 foaming/particle leaching technique, Journal of Applied Polymer Science, 133 (2016).

[28] E. Markočič, T. Botić, S. Kavčič, T. Bončina, Z. Knez, In vitro degradation of poly(d, l -lactide- co -glycolide) foams processed with supercritical fluids, Industrial and Engineering Chemistry Research, 54 (2015) 2114-2119.

[29] L. Diaz-Gomez, F. Yang, J. Jansen, A. Concheiro, C. alvarez-lorenzo, C.A. García-González, Low viscosity-PLGA scaffolds by compressed CO_2 foaming for growth factor delivery, RSC Advances, 6 (2016) 70510-70519.

[30] C. Yang, Y.-Q. Kang, X.-M. Liao, Y.-D. Yao, Z.-B. Huang, G.-F. Yin, Preparation of PLGA/β-TCP composite scaffolds with supercritical CO_2 foaming technique, Frontiers of Materials Science in China, 4 (2010) 314-320.

[31] L.I. Cabezas, V. Fernández, R. Mazarro, I. Gracia, A. De Lucas, J.F. Rodríguez, Production of biodegradable porous scaffolds impregnated with indomethacin in supercritical CO_2, Journal of Supercritical Fluids, 63 (2012) 155-160.

455 [32] L.I. Cabezas, I. Gracia, A. De Lucas, J.F. Rodríguez, Novel model for the description of the
456 controlled release of 5-fluorouracil from PLGA and PLA foamed scaffolds impregnated in
457 supercritical CO_2, Industrial and Engineering Chemistry Research, 53 (2014) 15374-15382.
458 [33] C. Gutiérrez, J.F. Rodríguez, I. Gracia, A. de Lucas, M.T. García, Foaming process from
459 polystyrene/p-cymene solutions using CO_2, Chemical Engineering and Technology, 37 (2014)
460 1845-1853.
461 [34] C. Gutiérrez, J.F. Rodríguez, I. Gracia, A. De Lucas, M.T. García, Preparation and
462 characterization of polystyrene foams from limonene solutions, Journal of Supercritical Fluids,
463 88 (2014) 92-104.
464 [35] I. Álvarez, C. Gutiérrez, A. de Lucas, J.F. Rodríguez, M.T. García, Measurement, correlation
465 and modelling of high-pressure phase equilibrium of PLGA solutions in CO_2, The Journal of
466 Supercritical Fluids, (2019) 104637.
467 [36] D. Villanueva Bermejo, E. Ibáñez, R.P. Stateva, T. Fornari, Solubility of CO_2 in Ethyl Lactate
468 and Modeling of the Phase Behavior of the CO_2 + Ethyl Lactate Mixture, Journal of Chemical &
469 Engineering Data, 58 (2013) 301-306.
470 [37] C. Gutiérrez, J.F. Rodríguez, I. Gracia, A. De Lucas, M.T. García, Development of a strategy
471 for the foaming of polystyrene dissolutions in $scCO_2$, Journal of Supercritical Fluids, 76 (2013)
472 126-134.
473 [38] J.-B. Bao, T. Liu, L. Zhao, G.-H. Hu, X. Miao, X. Li, Oriented foaming of polystyrene with
474 supercritical carbon dioxide for toughening, Polymer, 53 (2012) 5982-5993.
475 [39] C. Gutiérrez, M.T. Garcia, R. Mencía, I. Garrido, J.F. Rodríguez, Clean preparation of
476 tailored microcellular foams of polystyrene using nucleating agents and supercritical CO_2, Journal
477 of Materials Science, 51 (2016) 4825-4838.
478 [40] E. Aionicesei, M. Škerget, Ž. Knez, Measurement of CO_2 solubility and diffusivity in poly(l-
479 lactide) and poly(d,l-lactide-co-glycolide) by magnetic suspension balance, The Journal of
480 Supercritical Fluids, 47 (2008) 296-301.
481 [41] A. Kasturirangan, C.A. Koh, A.S. Teja, Glass-Transition Temperatures in CO_2 + Polymer
482 Systems: Modeling and Experiment, Industrial & Engineering Chemistry Research, 50 (2011)
483 158-162.
484 [42] D. Liu, D. Tomasko, Carbon dioxide sorption and dilation of poly(lactide-co-glycolide), The
485 Journal of supercritical fluids, 39 (2007) 416-425.
486 [43] R. Pini, G. Storti, M. Mazzotti, H. Tai, K.M. Shakesheff, S.M. Howdle, Sorption and swelling
487 of poly(DL-lactic acid) and poly(lactic-co-glycolic acid) in supercritical CO_2: An experimental
488 and modeling study, Journal of Polymer Science Part B: Polymer Physics, 46 (2008) 483-496.
489 [44] K. Toi, T. Nakamura, T. Ito, T. Kasai, Diffusion and sorption for carbon dioxide in Kapton
490 at extremely low pressure, Journal of applied polymer science, 69 (1998) 1013-1017.
491 [45] C.M. Stafford, T.P. Russell, T.J. McCarthy, Expansion of Polystyrene Using Supercritical
492 Carbon Dioxide: Effects of Molecular Weight, Polydispersity, and Low Molecular Weight
493 Components, Macromolecules, 32 (1999) 7610-7616.
494 [46] T.S. Chow, Molecular Interpretation of the Glass Transition Temperature of Polymer-Diluent
495 Systems, Macromolecules, 13 (1980) 362-364.
496 [47] J.S. Chiou, J.W. Barlow, D.R. Paul, Plasticization of glassy polymers by CO_2, Journal of
497 Applied Polymer Science, 30 (1985) 2633-2642.
498 [48] J. Reignier, J. Tatibouët, R. Gendron, Effect of dissolved carbon dioxide on the glass
499 transition and crystallization of poly(lactic acid) as probed by ultrasonic measurements, Journal
500 of Applied Polymer Science, 112 (2009) 1345-1355.
501 [49] D.J. Mooney, D.F. Baldwin, N.P. Suh, J.P. Vacanti, R. Langer, Novel approach to fabricate
502 porous sponges of poly(d,l-lactic-co-glycolic acid) without the use of organic solvents,
503 Biomaterials, 17 (1996) 1417-1422.
504 [50] D.W. Hutmacher, T. Schantz, I. Zein, K.W. Ng, S.H. Teoh, K.C. Tan, Mechanical properties
505 and cell cultural response of polycaprolactone scaffolds designed and fabricated via fused
506 deposition modeling, J Biomed Mater Res, 55 (2001) 203-216.
507 [51] M. Espanol, R.A. Perez, E.B. Montufar, C. Marichal, A. Sacco, M.P. Ginebra, Intrinsic
508 porosity of calcium phosphate cements and its significance for drug delivery and tissue
509 engineering applications, Acta Biomater, 5 (2009) 2752-2762.

510 [52] H. Tai, M.L. Mather, D. Howard, W. Wang, L.J. White, J.A. Crowe, S.P. Morgan, A.
511 Chandra, D.J. Williams, S.M. Howdle, K.M. Shakesheff, Control of pore size and structure of
512 tissue engineering scaffolds produced by supercritical fluid processing, European cells &
513 materials, 14 (2007) 64-77.
514 [53] E. Kiran, Foaming strategies for bioabsorbable polymers in supercritical fluid mixtures. Part
515 I. Miscibility and foaming of poly(l-lactic acid) in carbon dioxide+acetone binary fluid mixtures,
516 The Journal of Supercritical Fluids, 54 (2010) 296-307.
517 [54] A.B. Paninho, A.V.M. Nunes, A. Paiva, V. Najdanovic-Visak, High pressure phase behavior
518 of the binary system (ethyl lactate+carbon dioxide), Fluid Phase Equilibria, 360 (2013) 129-133.
519 [55] D.W. Cho, M.S. Shin, J. Shin, W. Bae, H. Kim, High-pressure phase behavior of methyl
520 lactate and ethyl lactate in supercritical carbon dioxide, Journal of Chemical and Engineering
521 Data, 56 (2011) 3561-3566.
522 [56] O.C. Onder, E. Yilgor, I. Yilgor, Critical parameters controlling the properties of monolithic
523 poly (lactic acid) foams prepared by thermally induced phase separation, Journal of Polymer
524 Science Part B: Polymer Physics, 57 (2019) 98-108.
525 [57] C. Gutiérrez, J.F. Rodríguez, I. Gracia, A. De Lucas, M.T. García, High-pressure phase
526 equilibria of Polystyrene dissolutions in Limonene in presence of CO_2, Journal of Supercritical
527 Fluids, 84 (2013) 211-220.
528 [58] A. Salerno, C. Domingo, Low-temperature clean preparation of poly(lactic acid) foams by
529 combining ethyl lactate and supercritical CO_2: correlation between processing and foam pore
530 structure, Polymer International, 63 (2014) 1303-1310.
531 [59] I. Tsivintzelis, A.G. Angelopoulou, C. Panayiotou, Foaming of polymers with supercritical
532 CO_2: An experimental and theoretical study, Polymer, 48 (2007) 5928-5939.
533 [60] E. Kiran, Modification of biomedical polymers in dense fluids. Miscibility and foaming of
534 poly(p-dioxanone) in carbon dioxide+acetone fluid mixtures, The Journal of Supercritical Fluids,
535 66 (2012) 372-379.
536 [61] L.M. Mathieu, M.O. Montjovent, P.E. Bourban, D.P. Pioletti, J.A.E. Månson, Bioresorbable
537 composites prepared by supercritical fluid foaming, Journal of Biomedical Materials Research
538 Part A, 75A (2005) 89-97.
539